

# Theory of Scalars

N.N. Achasov <sup>a</sup>, A.V. Kiselev <sup>a</sup>, and G.N. Shestakov <sup>a</sup>

<sup>a</sup>Laboratory of Theoretical Physics, S.L. Sobolev Institute for Mathematics, Academician Koptiug Prospekt, 4, Novosibirsk, 630090, Russia

Outline: 1. Introduction, 2. Confinement, chiral dynamics and light scalar mesons, 3. Chiral shielding of the  $\sigma(600)$ , chiral constraints (the CGL band), the  $\sigma(600)$  and the  $f_0(980)$  in  $\pi\pi \rightarrow \pi\pi$ ,  $\pi\pi \rightarrow K\bar{K}$ ,  $\phi \rightarrow \gamma\pi^0\pi^0$ , 4. The  $\phi$  meson radiative decays on light scalar resonances, 5. Light scalars in  $\gamma\gamma$  collisions.

Evidence for four-quark components of light scalars is given. The priority of Quantum Field Theory in revealing the light scalar mystery is emphasized.

## 1. Introduction

The scalar channels in the region up to 1 GeV became a stumbling block of QCD. The point is that both perturbation theory and sum rules do not work in these channels because there are not solitary resonances in this region.

At the same time the question on the nature of the light scalar mesons is major for understanding the mechanism of the chiral symmetry realization, arising from the confinement, and hence for understanding the confinement itself.

## 2. Place in QCD, chiral limit, confinement, and $\sigma$ models

The QCD Lagrangian is given by  $L = -\frac{1}{2}Tr(G_{\mu\nu}(x)G^{\mu\nu}(x)) + \bar{q}(x)(i\hat{D} - M)q(x)$ ,  $M$  is a diagonal matrix of quark masses,  $\hat{D} = \gamma^\mu D_\mu$ ,  $D_\mu = \partial_\mu + ig_0 G_\mu(x)$ .  $M$  mixes left and right spaces. But in chiral limit,  $M_{ff} \rightarrow 0$ , these spaces separate realize  $U_L(3) \times U_R(3)$  flavour symmetry, which, however, is broken by the gluonic anomaly up to  $U_{vec}(1) \times SU_L(3) \times SU_R(3)$ . As experiment suggests, confinement forms colourless observable hadronic fields and spontaneous breaking of chiral symmetry with massless pseudoscalar fields. There are two possible scenarios for QCD at low energy. 1. Non-linear  $\sigma$  model. 2. Linear  $\sigma$  model (LSM). The experimental nonet of the light scalar mesons,  $f_0(600)$  (or  $\sigma(600)$ ),  $\kappa(700-900)$ ,  $a_0(980)$  and  $f_0(980)$  mesons, suggests the  $U_L(3) \times U_R(3)$  LSM.

## 3. History

Hunting the light  $\sigma$  and  $\kappa$  mesons had begun in the sixties already and a preliminary information on the light scalar mesons in PDG Reviews had appeared at that time. But long-standing unsuccessful attempts to prove their existence in a conclusive way entailed general disappointment and an information on these states disappeared from PDG Reviews. One of principal reasons against the  $\sigma$  and  $\kappa$  mesons was the fact that both  $\pi\pi$  and  $\pi K$  scattering phase shifts do not pass over  $90^\circ$  at putative resonance masses.

## 4. $SU_L(2) \times SU_R(2)$ LSM, $\pi\pi \rightarrow \pi\pi$ [1,2,3]

Situation changes when we showed that in LSM there is a negative background phase which hides the  $\sigma$  meson in  $\pi\pi \rightarrow \pi\pi$ . It has been made clear that shielding wide lightest scalar mesons in chiral dynamics is very natural. This idea was picked up and triggered new wave of theoretical and experimental searches for the  $\sigma$  and  $\kappa$  mesons. Our approximation is as follows (see Fig. 1):

$$T_0^{0(tree)} = \frac{m_\pi^2 - m_\sigma^2}{32\pi f_\pi^2} \left[ 5 - 3 \frac{m_\sigma^2 - m_\pi^2}{m_\sigma^2 - s} - 2 \frac{m_\sigma^2 - m_\pi^2}{s - 4m_\pi^2} \right] \times \ln \left( 1 + \frac{s - 4m_\pi^2}{m_\sigma^2} \right), T_0^0 = T_0^{0(tree)} / [1 - i\rho_{\pi\pi}]$$

$$\times T_0^{0(tree)} = [e^{2i(\delta_{bg} + \delta_{res})} - 1] / (2i\rho_{\pi\pi}) = (e^{2i\delta_0^0} - 1) / (2i\rho_{\pi\pi}) = T_{bg} + e^{2i\delta_{bg}} T_{res}, T_{res} = [\sqrt{s}\Gamma_{res}(s)/\rho_{\pi\pi}] / [M_{res}^2 - s + \text{Re}\Pi_{res}(M_{res}^2) - \Pi_{res}(s)] = (e^{2i\delta_{res}} - 1) / (2i\rho_{\pi\pi}), T_{bg} = (e^{2i\delta_{bg}} - 1) / (2i\rho_{\pi\pi}) = \lambda(s) / [1 - i\rho_{\pi\pi}\lambda(s)], \lambda(s) = \frac{m_\pi^2 - m_\sigma^2}{32\pi f_\pi^2}$$

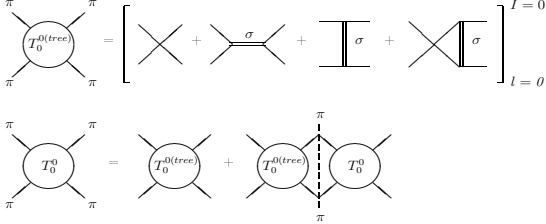


Figure 1. The graphical representation of the  $S$  wave  $I = 0$   $\pi\pi$  scattering amplitude  $T_0^0$ .

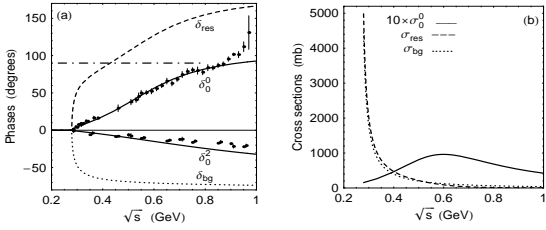


Figure 2. The  $\sigma$  model. Our approximation.  $\delta_0^0 = \delta_{res} + \delta_{bg}$ .  $(\sigma_0^0, \sigma_{res}, \sigma_{bg}) = 32\pi(|T_0^0|^2, |T_{res}|^2, |T_{bg}|^2)/s$ .

$$\begin{aligned} & \times \left[ 5 - 2 \frac{m_\sigma^2 - m_\pi^2}{s - 4m_\pi^2} \ln \left( 1 + \frac{s - 4m_\pi^2}{m_\sigma^2} \right) \right], f_\pi = 92.4 \text{ MeV}, \\ & \text{Re}\Pi_{res}(s) = -g_{res}^2(s) \lambda(s) \rho_{\pi\pi}^2 / (16\pi), \text{Im}\Pi_{res}(s) = \\ & g_{res}^2(s) \rho_{\pi\pi} / (16\pi), g_{res}(s) = g_{\sigma\pi\pi} / |1 - i\rho_{\pi\pi} \lambda(s)|, \\ & M_{res}^2 = m_\sigma^2 - \text{Re}\Pi_{res}(M_{res}^2), \rho_{\pi\pi} = (1 - 4m_\pi^2/s)^{1/2}, \\ & g_{\sigma\pi\pi} = (3/2)^{1/2} g_{\sigma\pi^+\pi^-} = (3/2)^{1/2} (m_\pi^2 - m_\sigma^2) / f_\pi. \\ & T_0^2(\text{tree}) = \frac{m_\pi^2 - m_\sigma^2}{16\pi f_\pi^2} \left[ 1 - \frac{m_\sigma^2 - m_\pi^2}{s - 4m_\pi^2} \ln \left( 1 + \frac{s - 4m_\pi^2}{m_\sigma^2} \right) \right], \\ & T_0^2 = T_0^2(\text{tree}) / [1 - i\rho_{\pi\pi} T_0^2(\text{tree})] = \frac{\epsilon^{2i\delta_0^0} - 1}{2i\rho_{\pi\pi}}. \end{aligned}$$

### 5. Results in our approximation [3].

$$\begin{aligned} & M_{res} = 0.43 \text{ GeV}, \Gamma_{res}(M_{res}^2) = 0.67 \text{ GeV}, \\ & m_\sigma = 0.93 \text{ GeV}, \Gamma_{res}^{\text{norm}}(M_{res}^2) = \Gamma_{res}(M_{res}^2) / (1 + \\ & d\text{Re}\Pi_{res}(s)/ds|_{s=M_{res}^2}) = 0.53 \text{ GeV}, \Gamma_{res}(s) = \\ & \frac{g_{res}^2(s)}{16\pi\sqrt{s}} \rho_{\pi\pi}, g_{res}(M_{res}^2) / g_{\sigma\pi\pi} = 0.33, a_0^0 = 0.18 m_\pi^{-1}, \\ & a_0^2 = -0.04 m_\pi^{-1}, (s_A)_0^0 = 0.45 m_\pi^2, (s_A)_0^2 = 2.02 m_\pi^2. \end{aligned}$$

### 6. Chiral shielding in $\pi\pi \rightarrow \pi\pi$ [3]

The chiral shielding of the  $\sigma(600)$  meson is illustrated in Fig. 2(a) with the help of the  $\pi\pi$  phase shifts  $\delta_{res}$ ,  $\delta_{bg}$ , and  $\delta_0^0$ , and in Fig. 2(b) with the help of the corresponding cross sections.

### 7. The $\sigma$ pole in $\pi\pi \rightarrow \pi\pi$ [3]

$$\begin{aligned} & T_0^0 \rightarrow g_\pi^2 / (s - s_R), g_\pi^2 = (0.12 + i0.21) \text{ GeV}^2, \\ & \sqrt{s_R} = M_R - i\Gamma_R/2 = (0.52 - i0.25) \text{ GeV}. \end{aligned}$$

Considering the residue of the  $\sigma$  pole in  $T_0^0$  as the square of its coupling constant to the  $\pi\pi$  channel is not a clear guide to understand the  $\sigma$  meson nature for its great obscure imaginary part.

### 8. The $\sigma$ propagator [3]

$$1/D_\sigma(s) = 1/[M_{res}^2 - s + \text{Re}\Pi_{res}(M_{res}^2) - \Pi_{res}(s)].$$

The  $\sigma$  meson self-energy  $\Pi_{res}(s)$  is caused by the intermediate  $\pi\pi$  states, that is, by the four-quark intermediate states if we keep in mind that the  $SU_L(2) \times SU_R(2)$  LSM could be the low energy realization of the two-flavour QCD. This contribution shifts the Breit-Wigner (BW) mass greatly  $m_\sigma - M_{res} = 0.50 \text{ GeV}$ . So, half the BW mass is determined by the four-quark contribution at least. The imaginary part dominates the propagator modulus in the region  $300 \text{ MeV} < \sqrt{s} < 600 \text{ MeV}$ . So, the  $\sigma$  field is described by its four-quark component at least in this energy region.

### 9. Chiral shielding in $\gamma\gamma \rightarrow \pi\pi$ [3]

$$\begin{aligned} & T_S(\gamma\gamma \rightarrow \pi^+\pi^-) = T_S^{\text{Born}}(\gamma\gamma \rightarrow \pi^+\pi^-) \\ & \quad + 8\alpha I_{\pi^+\pi^-} T_S(\pi^+\pi^- \rightarrow \pi^+\pi^-) \\ & = T_S^{\text{Born}}(\gamma\gamma \rightarrow \pi^+\pi^-) + \frac{8\alpha}{3} I_{\pi^+\pi^-} (2T_0^0 + T_0^2), \\ & T_S(\gamma\gamma \rightarrow \pi^0\pi^0) = 8\alpha I_{\pi^+\pi^-} T_S(\pi^+\pi^- \rightarrow \pi^0\pi^0) \\ & \quad = 16\alpha I_{\pi^+\pi^-} (T_0^0 - T_0^2)/3, \\ & I_{\pi^+\pi^-} = \frac{m_\pi^2}{s} (\pi + i \ln \frac{1 + \rho_{\pi\pi}}{1 - \rho_{\pi\pi}})^2 - 1, \quad s \geq 4m_\pi^2, \\ & T_S^{\text{Born}}(\gamma\gamma \rightarrow \pi^+\pi^-) = (8\alpha/\rho_{\pi^+\pi^-}) \text{Im}I_{\pi^+\pi^-}. \end{aligned}$$

Our results are shown in Fig. 3.

$\Gamma(\sigma \rightarrow \pi^+\pi^- \rightarrow \gamma\gamma, s) = \frac{1}{16\pi\sqrt{s}} |g(\sigma \rightarrow \pi^+\pi^- \rightarrow \gamma\gamma, s)|^2$ , where  $g(\sigma \rightarrow \pi^+\pi^- \rightarrow \gamma\gamma, s) = (\alpha/2\pi) \times I_{\pi^+\pi^-} g_{res} \pi^+\pi^-(s)$ ; see Fig. 4. So, the  $\sigma \rightarrow \gamma\gamma$  decay is described by the triangle  $\pi^+\pi^-$  loop diagram  $res \rightarrow \pi^+\pi^- \rightarrow \gamma\gamma$ . Consequently, it is due to the four-quark transition because we imply a low energy realization of the two-flavour QCD by means of the the  $SU_L(2) \times SU_R(2)$  LSM. As Fig. 4 suggests, the real intermediate  $\pi^+\pi^-$  state dominates in  $g(res \rightarrow \pi^+\pi^- \rightarrow \gamma\gamma)$  in the  $\sigma$  region  $\sqrt{s} < 0.6 \text{ GeV}$ . Thus the picture in the physical region is clear and informative. But, what about the pole in the complex  $s$  plane? Does

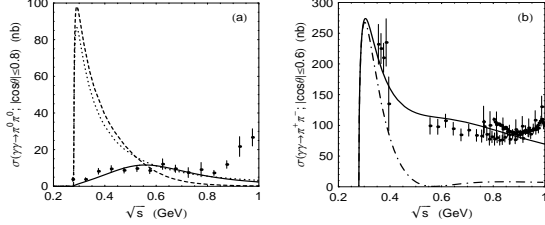


Figure 3. (a) The solid, dashed, and dotted lines are  $\sigma_S(\gamma\gamma \rightarrow \pi^0\pi^0)$ ,  $\sigma_{res}(\gamma\gamma \rightarrow \pi^0\pi^0)$ , and  $\sigma_{bg}(\gamma\gamma \rightarrow \pi^0\pi^0)$ . (b) The dashed-dotted line is  $\sigma_S(\gamma\gamma \rightarrow \pi^+\pi^-)$ , the solid line includes the higher waves from  $T^{Born}(\gamma\gamma \rightarrow \pi^+\pi^-)$ .

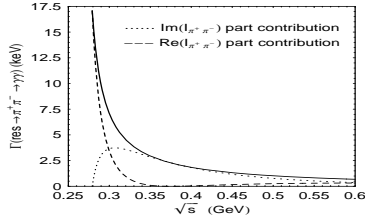


Figure 4. The energy dependent width of the  $\sigma \rightarrow \pi^+\pi^-\gamma$  decay.

the pole residue reveal the  $\sigma$  indeed?

## 10. The $\sigma$ pole in $\gamma\gamma \rightarrow \pi\pi$ [3]

$\frac{1}{16\pi}\sqrt{\frac{3}{2}}T_S(\gamma\gamma \rightarrow \pi^0\pi^0) \rightarrow g_\gamma g_\pi/(s - s_R)$ ,  
 $g_\gamma g_\pi = (-0.45 - i0.19) \cdot 10^{-3} \text{ GeV}^2$ ,  $g_\gamma/g_\pi = (-1.61 + i1.21) \cdot 10^{-3}$ ,  $\Gamma(\sigma \rightarrow \gamma\gamma) = \frac{|g_\gamma|^2}{M_R} \approx 2 \text{ keV}$ .  
 It is hard to believe that anybody could learn the complex but physically clear dynamics of the  $\sigma \rightarrow \gamma\gamma$  decay from the residues of the  $\sigma$  pole.

## 11. Discussion [3,4,5,6]

Leutwyler and collaborators obtained  $\sqrt{s_R} = M_R - i\Gamma_R/2 = (441_{-8}^{+16} - i272_{-9}^{+12.5}) \text{ MeV}$  with the help of the Roy equation. Our result agrees with the above only qualitatively.  $\sqrt{s_R} = M_R - i\Gamma_R/2 = (518 - i250) \text{ MeV}$ . This is natural, because our approximation gives only a semiquantitative description of the data at  $\sqrt{s} < 0.4 \text{ GeV}$ . We do not regard also for effects of the  $K\bar{K}$  channel, the  $f_0(980)$  meson, and so on, that is, do not

consider the  $SU_L(3) \times SU_R(3)$  LSM.

Could the above scenario incorporates the primary lightest scalar Jaffe four-quark state? Certainly the direct coupling of this state to  $\gamma\gamma$  via neutral vector pairs ( $\rho^0\rho^0$  and  $\omega\omega$ ), contained in its wave function, is negligible,  $\Gamma(q^2\bar{q}^2 \rightarrow \rho^0\rho^0 + \omega\omega \rightarrow \gamma\gamma) \approx 10^{-3} \text{ keV}$ , as we showed in 1982 [6]. But its coupling to  $\pi\pi$  is strong and leads to  $\Gamma(q^2\bar{q}^2 \rightarrow \pi^+\pi^- \rightarrow \gamma\gamma)$  similar to  $\Gamma(res \rightarrow \pi^+\pi^- \rightarrow \gamma\gamma)$  in the above Fig. 4.

Let us add to  $T_S(\gamma\gamma \rightarrow \pi^0\pi^0)$  the amplitude for the the direct coupling of  $\sigma$  to  $\gamma\gamma$  conserving unitarity  $T_{direct}(\gamma\gamma \rightarrow \pi^0\pi^0) = sg_{\sigma\gamma\gamma}^{(0)}g_{res}(s)e^{i\delta_{bg}}/D_{res}(s)$ , where  $g_{\sigma\gamma\gamma}^{(0)}$  is the direct coupling constant of  $\sigma$  to  $\gamma\gamma$ , the factor  $s$  is caused by gauge invariance. Fitting the  $\gamma\gamma \rightarrow \pi^0\pi^0$  data gives a negligible value of  $g_{\sigma\gamma\gamma}^{(0)}$ ,  $\Gamma_{\sigma\gamma\gamma}^{(0)} = |M_{res}^2 g_{\sigma\gamma\gamma}^{(0)}|^2 / (16\pi M_{res}) \approx 0.0034 \text{ keV}$ , in astonishing agreement with our prediction [6].

The majority of current investigations of the mass spectra in scalar channels do not study particle production mechanisms. Because of this, such investigations are essentially preprocessing experiments, and the derivable information is very relative. Nevertheless, the progress in understanding the particle production mechanisms could essentially help us reveal the light scalar meson nature.

## 12. Troubles and expectancies

In theory the principal problem is impossibility to use the linear  $\sigma$  model in the tree level approximation inserting widths into  $\sigma$  meson propagators because such an approach breaks the both unitarity and Adler self-consistency conditions. Strictly speaking, the comparison with the experiment requires the non-perturbative calculation of the process amplitudes. Nevertheless, now there are the possibilities to estimate odds of the  $U_L(3) \times U_R(3)$  LSM to underlie physics of light scalar mesons in phenomenology. Really, even now there is a body of information about the  $S$  waves of different two-particle pseudoscalar states. As for theory, we know quite a lot about the scenario under discussion: the nine scalar mesons, the putative chiral shielding of the  $\sigma(600)$  and  $\kappa(700-900)$  mesons, the unitarity, an-

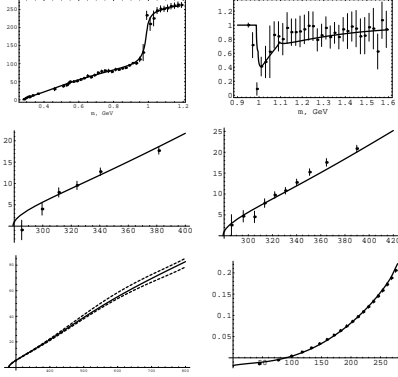


Figure 5. The phenomenological chiral shielding.  $\delta_0^0 = \delta_B^{\pi\pi} + \delta_{res}$ . The comparison with the CERN-Munich data for  $\delta_0^0$  and inelasticity  $\eta_0^0$ , with the BNL and NA48 data for  $\delta_0^0$ , with the CGL band for  $\delta_0^0$  [8], and with Leutwyler's calculation of  $T_0^0$  for  $s < 4m_\pi^2$ , respectively.

alyticity and Adler self-consistency conditions. In addition, there is the light scalar meson treatment motivated by field theory.

### 13. Phenomenological chiral shielding [7]

$g_{\sigma\pi^+\pi^-}^2/4\pi = 0.99 \text{ GeV}^2$ ,  $g_{\sigma K^+K^-}^2/4\pi = 2 \cdot 10^{-4} \text{ GeV}^2$ ,  $g_{f_0\pi^+\pi^-}^2/4\pi = 0.12 \text{ GeV}^2$ ,  $g_{f_0K^+K^-}^2/4\pi = 1.04 \text{ GeV}^2$ . The BW masses and width:  $m_{f_0} = 989 \text{ MeV}$ ,  $m_\sigma = 679 \text{ MeV}$ ,  $\Gamma_\sigma = 498 \text{ MeV}$ . The  $l=I=0$   $\pi\pi$  scattering length  $a_0^0 = 0.223 m_{\pi^+}^{-1}$ . Figure 5 illustrates the excellent agreement our phenomenological treatment with the experimental and theoretical data.

### 14. Four-quark model [5,9,10]

The nontrivial nature of the well-established light scalar resonances  $f_0(980)$  and  $a_0(980)$  is no longer denied practically anybody. In particular, there exist numerous evidences in favour of the  $q^2\bar{q}^2$  structure of these states. As for the nonet as a whole, even a dope's look at PDG Review gives an idea of the four-quark structure of the light scalar meson nonet,<sup>1</sup>  $\sigma(600)$ ,  $\kappa(700-900)$ ,

<sup>1</sup>To be on the safe side, notice that LSM does not contradict to non- $q\bar{q}$  nature of the low lying scalars because Quantum Fields can contain different virtual particles in

$a_0(980)$ , and  $f_0(980)$ , inverted in comparison with the classical  $P$  wave  $q\bar{q}$  tensor meson nonet  $a_2(1270)$ ,  $f_2(1320)$ ,  $K_2^*(1420)$ , and  $f_2'(1525)$ . Really, while the scalar nonet cannot be treated as the  $P$  wave  $q\bar{q}$  nonet in the naive quark model, it can be easily understood as the  $q^2\bar{q}^2$  nonet, where  $\sigma(600)$  has no strange quarks,  $\kappa(700-900)$  has the  $s$  quark,  $a_0(980)$  and  $f_0(980)$  have the  $s\bar{s}$  pair. The scalar mesons  $a_0(980)$  and  $f_0(980)$ , discovered more than thirty years ago, became the hard problem for the naive  $q\bar{q}$  model from the outset. Really, on the one hand, the almost exact degeneration of the masses of the isovector  $a_0(980)$  and isoscalar  $f_0(980)$  states revealed seemingly the structure similar to the structure of the vector  $\rho$  and  $\omega$  or tensor  $a_2(1320)$  and  $f_2(1270)$  mesons, but on the other hand, the strong coupling of  $f_0(980)$  to  $K\bar{K}$  suggests a considerable  $s\bar{s}$  part in the  $f_0(980)$  wave function.

In 1977 Jaffe noted that in the MIT bag model, which incorporates confinement phenomenologically, there are light four-quark scalar states. He suggested also that  $a_0(980)$  and  $f_0(980)$  might be these states. From that time  $a_0(980)$  and  $f_0(980)$  resonances came into beloved children of the light quark spectroscopy.

### 15. Radiative decays of $\phi$ meson [9,10,11,12,13]

Ten years later we showed [11] that the study of the radiative decays  $\phi \rightarrow \gamma a_0 \rightarrow \gamma\pi\eta$  and  $\phi \rightarrow \gamma f_0 \rightarrow \gamma\pi\pi$  can shed light on the problem of  $a_0(980)$  and  $f_0(980)$  mesons. Over the next ten years before experiments (1998) the question was considered from different points of view. Now these decays have been studied not only theoretically but also experimentally. The first measurements were reported by SND and CMD-2. More recently KLOE performed measurements which are in close agreement with the Novosibirsk data but have considerably smaller errors. Note that  $a_0(980)$  is produced in the radiative  $\phi$  meson decay as intensively as  $\eta'(958)$  containing  $\approx 66\%$  of  $s\bar{s}$ , responsible for  $\phi \approx s\bar{s} \rightarrow \gamma s\bar{s} \rightarrow \gamma\eta'(958)$ . It is a clear qualitative argument for the presence of the  $s\bar{s}$  pair in the isovector  $a_0(980)$  state, i.e., for different regions of virtuality.

its four-quark nature.

### 16. $K^+K^-$ loop mechanism of creation, spectra, and gauge invariance [7,9,10, 11,12,13,14]

When basing the experimental investigations, we suggested [11] one-loop model  $\phi \rightarrow K^+K^- \rightarrow \gamma a_0(980)$  (or  $f_0(980)$ ); see Fig. 6. This model is used in the data treatment and is ratified by experiment. Below we argue on gauge invariance grounds that the present data give the conclusive arguments in favor of the  $K^+K^-$  loop transition as the principal mechanism of  $a_0(980)$  and  $f_0(980)$  production in the  $\phi$  radiative decays. This enables to conclude that production of the lightest scalars  $a_0(980)$  and  $f_0(980)$  in these decays is caused by the four-quark transitions, resulting in strong restrictions on the large  $N_C$  expansions of the decay amplitudes. The analysis shows that these constraints give new evidences in favor of the four-quark nature of  $a_0(980)$  and  $f_0(980)$  mesons. The data are described in the model  $\phi \rightarrow (\gamma a_0 + \pi^0 \rho) \rightarrow \gamma \pi^0 \eta$  and  $\phi \rightarrow [\gamma(f_0 + \sigma) + \pi^0 \rho] \rightarrow \gamma \pi^0 \pi^0$ ; see Figs. 7.

To describe the experimental spectra  $dBR(\phi \rightarrow \gamma R \rightarrow \gamma ab, m)/dm = |g_R(m)|^2 \omega(m) p_{ab}(m) |g_{Rab}/D_R(m)|^2 / (\Gamma_\phi 48\pi^3 m_\phi^2)$ ,  $R = a_0, f_0$ ,  $ab = \pi^0 \eta, \pi^0 \pi^0$ , the function  $|g_R(m)|^2$  should be smooth (almost constant) for  $m \leq 0.99$  GeV. But the problem issues from gauge invariance which requires that  $g_R(m)$  is proportional to the photon energy  $\omega(m) = (m_\phi^2 - m^2)/2m_\phi$  (at least!) in the soft photon region. Stopping the function  $(\omega(m))^2$  at  $\omega(990 \text{ MeV}) = 29 \text{ MeV}$  with the help of the form-factor  $1/[1 + (R\omega(m))^2]$  requires a prohibitive  $R \approx 100 \text{ GeV}^{-1}$ .  $R \approx 10 \text{ GeV}^{-1}$  allows us to obtain the maximum of the mass spectrum only near 900 MeV. The  $K^+K^-$  loop model  $\phi \rightarrow K^+K^- \rightarrow \gamma R$  solves this problem in the elegant way: a fine threshold phenomenon is discovered, see Fig. 8.

### 17. $K^+K^-$ loop mechanism [10,13]

In truth this means that  $a_0(980)$  and  $f_0(980)$  are seen in the radiative decays of  $\phi$  meson owing to  $K^+K^-$  intermediate state. So, the mechanism of production of  $a_0(980)$  and  $f_0(980)$  mesons in

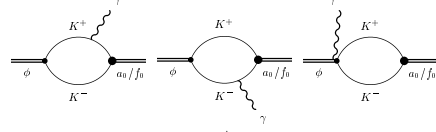


Figure 6. The  $K^+K^-$  loop model.

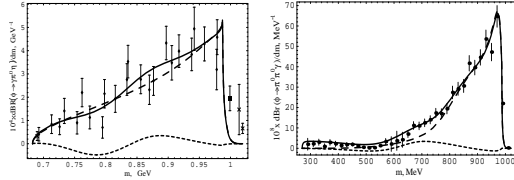


Figure 7. The left (right) plot illustrates the fit to the KLOE data for the  $\pi^0 \eta$  ( $\pi^0 \pi^0$ ) mass spectrum in the  $\phi \rightarrow \gamma \pi^0 \eta$  ( $\phi \rightarrow \gamma \pi^0 \pi^0$ ) decay.

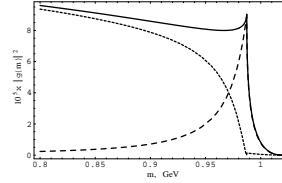


Figure 8. A new threshold phenomenon in  $\phi \rightarrow K^+K^- \rightarrow \gamma R$  decays. The universal in  $K^+K^-$  loop model function  $|g(m)|^2 = |g_R(m)/g_{RK^+K^-}|^2$  is drawn with the solid line. The contributions of the imaginary and real parts of  $g(m)$  are drawn with the dashed and dotted lines, respectively.

the  $\phi$  radiative decays is established at a physical level of proof. The real part of the  $\phi \rightarrow \gamma R$  amplitude contains two different contribution. One is caused by intermediate momenta (a few GeV) in the loops and the other is caused by super high momenta in the loops. At  $\omega(m) = 0$  these contribution eliminate each other. With increasing  $\omega(m)$  the contribution from intermediate momenta decreases rapidly enough. The contribution from super high momenta is constant and causes the  $\phi \rightarrow \gamma R$  amplitude in a great part.

### 18. Four-quark transition and OZI [10]

Both real and imaginary parts of the  $\phi \rightarrow \gamma R$  amplitude are caused by the  $K^+K^-$  intermediate state. The imaginary part is caused by the real  $K^+K^-$  state while the real part is caused by the

virtual compact  $K^+K^-$  state, i.e., we are dealing here with the four-quark transition. Needless to say, radiative four-quark transitions can happen between two  $q\bar{q}$  states as well as between  $q\bar{q}$  and  $q^2\bar{q}^2$  states but their intensities depend strongly on a type of the transitions. A radiative four-quark transition between two  $q\bar{q}$  states requires creation and annihilation of an additional  $q\bar{q}$  pair, i.e., such a transition is forbidden according to the Okubo-Zweig-Iizuka (OZI) rule, while a radiative four-quark transition between  $q\bar{q}$  and  $q^2\bar{q}^2$  states requires only creation of an additional  $q\bar{q}$  pair, i.e., such a transition is allowed according to the OZI rule. The consideration of this problem from the large  $N_C$  expansion standpoint supports the suppression of a radiative four-quark transition between two  $q\bar{q}$  states in comparison with a radiative four-quark transition between  $q\bar{q}$  and  $q^2\bar{q}^2$  states.

### 19. $a_0(980)/f_0(980) \rightarrow \gamma\gamma$ & $q^2\bar{q}^2$ model

Recall that twenty six years ago the suppression of  $a_0(980)/f_0(980) \rightarrow \gamma\gamma$  was predicted [6,15] based on the  $q^2\bar{q}^2$  model,  $\Gamma(a_0(980)/f_0(980) \rightarrow \gamma\gamma) \sim 0.27$  keV. Experiment supported this prediction  $\Gamma(a_0 \rightarrow \gamma\gamma) = (0.19 \pm 0.07^{+0.1}_{-0.07})/B(a_0 \rightarrow \pi\eta)$  keV, Crystal Ball, and  $(0.28 \pm 0.04 \pm 0.1)/B(a_0 \rightarrow \pi\eta)$  keV, JADE,  $\Gamma(f_0 \rightarrow \gamma\gamma) = (0.31 \pm 0.14 \pm 0.09)$  keV, Crystal Ball, and  $(0.24 \pm 0.06 \pm 0.15)$  keV, MARK II. When in the  $q\bar{q}$  model it was anticipated  $\Gamma(a_0 \rightarrow \gamma\gamma) = (1.5-5.9)\Gamma(a_2 \rightarrow \gamma\gamma) = (1.5-5.9)(1.04 \pm 0.09)$  keV and  $\Gamma(f_0 \rightarrow \gamma\gamma) = (1.7-5.5)\Gamma(f_2 \rightarrow \gamma\gamma) = (1.7-5.5)(2.8 \pm 0.4)$  keV. The  $a_0 \rightarrow K^+K^- \rightarrow \gamma\gamma$  model [16] describes adequately data and corresponds to the four-quark transition  $a_0 \rightarrow q^2\bar{q}^2 \rightarrow \gamma\gamma$ ,  $\langle \Gamma(a_0 \rightarrow K^+K^- \rightarrow \gamma\gamma) \approx 0.3$  keV.

### 20. $\gamma\gamma \rightarrow \pi\pi$ from Belle [17,18,19]

Recently, we analyzed the new high statistics Belle data on the reactions  $\gamma\gamma \rightarrow \pi^+\pi^-$  and  $\gamma\gamma \rightarrow \pi^0\pi^0$ , and clarified the current situation around the  $\sigma(600)$ ,  $f_0(980)$ , and  $f_2(1270)$  resonances in  $\gamma\gamma$  collisions. The new Belle data are shown in Fig. 9, together with our fitted curves. The  $f_0 \rightarrow K^+K^- \rightarrow \gamma\gamma$  approximation

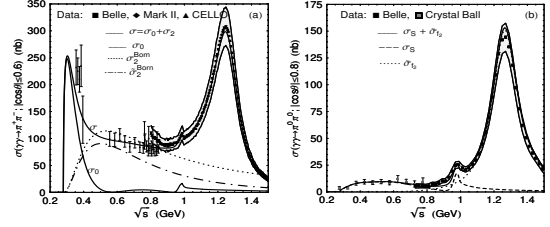


Figure 9. (a) Cross section for  $\gamma\gamma \rightarrow \pi^+\pi^-$ . (b) Cross section for  $\gamma\gamma \rightarrow \pi^0\pi^0$ .

yields  $\langle \Gamma_{f_0 \rightarrow K^+K^- \rightarrow \gamma\gamma} \rangle \approx 0.2$  keV. The direct couplings  $\sigma \rightarrow \gamma\gamma$  and  $f_0 \rightarrow \gamma\gamma$  are small:  $\Gamma_{\sigma \rightarrow \gamma\gamma}^{direct} \ll 0.1$  keV,  $\Gamma_{f_0 \rightarrow \gamma\gamma}^{direct} \ll 0.1$  keV.

We thank Heiri Leutwyler very much for communications. This work was supported in part by the Presidential Grant No. NSh-1027.2008.2 and by the RFFI Grant No. 07-02-00093.

## REFERENCES

1. M. Gell-Mann and M. Levy, *Nuovo Cimento* **16**, 705 (1960).
2. N.N. Achasov and G.N. Shestakov, *Phys. Rev. D* **49**, 5779(1994).
3. N.N. Achasov and G.N. Shestakov, *Phys. Rev. Lett.* **99**, 072001 (2007).
4. I. Caprini, G. Colangelo, and H. Leutwyler, *Phys. Rev. Lett.* **96**, 132001 (2006).
5. R.L. Jaffe, *Phys. Rev. D* **15**, 267, 281 (1977).
6. N.N. Achasov et al., *Phys. Lett.* **108B**, 134 (1982); *Z. Phys. C* **16**, 55 (1982).
7. N.N. Achasov and A.V. Kiselev, *Phys. Rev. D* **73**, 054029 (2006); *Yad.Fiz.* **70**, 2005 (2007).
8. G. Colangelo, J. Gasser, and H. Leutwyler, *Nucl. Phys. B* **603**, 125 (2001).
9. N.N. Achasov, *Yad.Fiz.* **65**, 573 (2002).
10. N.N. Achasov, *Nucl. Phys. A* **728**, 425 (2003).
11. N.N. Achasov and V.N. Ivanchenko, *Nucl. Phys. B* **315** (1989) 465.
12. N.N. Achasov and V.V. Gubin, *Phys. Rev. D* **56**, 4084 (1997).
13. N.N. Achasov and V.V. Gubin, *Phys. Rev. D* **63**, 094007 (2001).
14. N.N. Achasov and A.V. Kiselev, *Phys. Rev. D* **68**, 014006 (2003).
15. N.N. Achasov et al., *Z. Phys. C* **27**, 99 (1985).
16. N.N. Achasov, and G.N. Shestakov, *Z. Phys. C* **41**, 309 (1988).
17. T. Mori et al., *J. Phys. Soc. Jap.* **76**, 074102 (2007); K. Abe et al., arXiv: 0711.1926 [hep-ex].
18. N.N. Achasov and G.N. Shestakov, *Phys. Rev. D* **72**, 013006 (2005).

19. N.N. Achasov and G.N. Shestakov, *Phys. Rev. D* **77**, 074020 (2008).